

Preparation of Poly(4-phthalimide) Nanoribbon by Reaction-Induced Crystallization

Kanji Wakabayashi,[†] Tetsuya Uchida,[‡] Shinichi Yamazaki, and Kunio Kimura^{*,†}

Graduate School of Environmental Science and Graduate School of Natural Science and Technology, Okayama University, 3-1-1 Tsushima-naka Okayama, Japan 700-8530

Received April 20, 2008

ABSTRACT: The morphology of poly(4-phthalimide) (PPI) crystals was examined by using reaction-induced crystallization of oligomers during solution polymerization. Polymerizations of alkyl 4-aminophthalates such as 1-ethyl 4-aminophthalate (1EAP), 2-ethyl 4-aminophthalate, 1-hexyl 4-aminophthalate, and 2-hexyl 4-aminophthalate were carried out at 330 °C in a mixture of isomers of dibenzyltoluene without stirring. Nanoscale PPI ribbons having smooth surface were formed by the polymerizations of these monomers. The ribbons prepared from 1EAP at a concentration of 2.0% for 24 h were averagely 12 μm in length, 150 nm in width, and 8 nm in thickness, in which the molecular chains aligned along the long axis of the ribbon. The phase-separated oligomers were fully cyclized imide oligomers, and this is of great importance for the formation of the ribbon. The obtained ribbons possessed high crystallinity and exhibited excellent thermal stability.

Introduction

Aromatic polyimides have been representative of high-performance polymers with prominent thermal stability, mechanical properties, chemical stability, low conductivity, and so on. Although some aromatic polyimides containing flexible moieties, bulky groups, or irregular structure as comonomers exhibit fusibility and solubility,^{1,2} many of the rigid-rod aromatic polyimides are intractable. Morphology and molecular orientation are of great importance to control the properties of materials, and desirable morphology and molecular orientation are necessary to obtain ultimate properties expected from the polymer structure. The intractability of the rigid-rod polyimides makes them difficult to control the morphology and the molecular orientation. Polyimides has been usually prepared by a two-step procedure including the synthesis of soluble poly(amic acid) precursors and the following imidization.^{1,2} The difficulty of the molecular chain orientation of poly(amic acid) precursors caused from the catenation and the rapid crystallization during imidization prevents from controlling the morphology and the molecular chain orientation of polyimides.

Isothermal polymerizations can induce phase separation from homogeneous solution.^{3–8} The phase separation is determined by miscibility of the oligomer and the solvent being related to the decrease of solution mixing entropy. The interplay between the polymerization and the phase separation is responsible for the phase separation modes including crystallization and liquid–liquid phase separation. Hence, the reaction-induced phase separation has been extensively studied to control the morphology by tuning the polymerization conditions.^{9,10} We have been studying the morphology control of poly(*p*-phenylene pyromellitimide) by using the phase separation during polymerization, and lozenge-shaped crystal and microspheres were obtained.^{11,12} Poly(4-phthalimide) (PPI) is a rigid-rod aromatic polyimide, and it had also been a hopeful candidate of high-performance materials. PPI was previously synthesized by the polymerization of 4-aminophthalic anhydride.^{13,14} However, the purification of the monomer was quite difficult because 4-aminophthalic anhydride rapidly self-polymerized. Because

of this instability of the monomer, the high molecular weight PPI had not been obtained. PPI was also synthesized by the electropolymerization of 4-aminophthalic acid.¹⁵ Although dark amber films were obtained, the molecular weight was low. These studies are interesting, but high molecular weight PPI had not been prepared. Further, the study on the morphology control of PPI had not been examined.

In this paper, morphology control of PPI was examined by using the reaction-induced crystallization of oligomers during solution polymerization of 1- and 2-alkyl 4-aminophthalates as depicted in Scheme 1.

Experimental Section

Materials. 4-Nitrophthalic anhydride was obtained from Tokyo Kasei Co. Ltd. and recrystallized from acetic anhydride. The mixture of isomeric dibenzyltoluene (DBT) was obtained from Matsumura Oil Co. Ltd. (trade name: Barrel Therm 400; MW 270, bp 390 °C) and distilled under reduced pressure (170–175 °C, 0.3 mmHg).

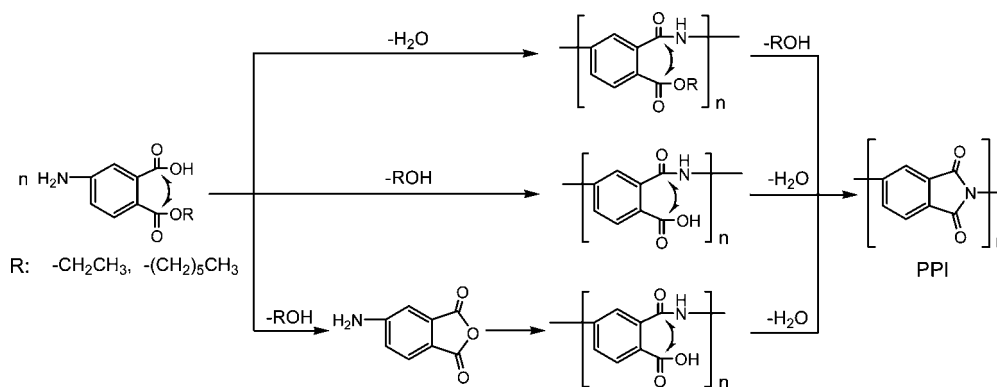
Measurements. Morphology of the products was observed on a HITACHI S-3500N scanning electron microscope (SEM). Samples were dried, sputtered with platinum/palladium, and observed at 20 kV. Average shape parameters of the products were determined by taking the average of over 150 observation values. Morphology of the products and a selected-area electron diffraction (ED) were observed on a JEOL 2000EX transmission electron microscope (TEM) at 200 kV. Atomic force microscopy image was taken on a Digital Instruments, Inc. Nanoscope IIIa in air. ¹H NMR spectra were recorded on a JEOL JNM-AL spectrometer operating at 300 MHz. A solid-state ¹³C NMR spectrum was measured on a Bruker AVANCE300WB spectrometer operating at 75 MHz. Infrared (IR) spectra were recorded on a JASCO FT/IR-410 spectrometer. A powder pattern of wide-angle X-ray scattering (WAXS) was recorded on a RIGAKU MiniFlex diffractometer with nickel-filtered Cu K α radiation at 30 kV and 15 mA with a scanning rate of 1° min⁻¹. Matrix-assisted laser desorption/ionization time-of-flight (MALDI-TOF) mass spectrometry was performed on a Bruker Daltonics AutoFLEX MALDI-TOF MS system operating with a 337 nm N₂ laser. Spectra were obtained in the linear positive mode with accelerating potential of 20 kV. Mass was calibrated with angiotensin I (MW 1296.69) and insulin B (MW 3496.96) of a Sequazyme peptide mass standard kit. Samples were prepared by the evaporation-grinding method and then measured in 3-aminoquinoline and dithranol as a matrix doped with potassium trifluoroacetate salt according to the procedure.¹⁷ Thermogravimetric analysis (TGA) was performed on a Perkin-Elmer TGA-7 with a

* To whom correspondence should be addressed: Tel and Fax +81-86-251-8902; e-mail polykim@cc.okayama-u.ac.jp.

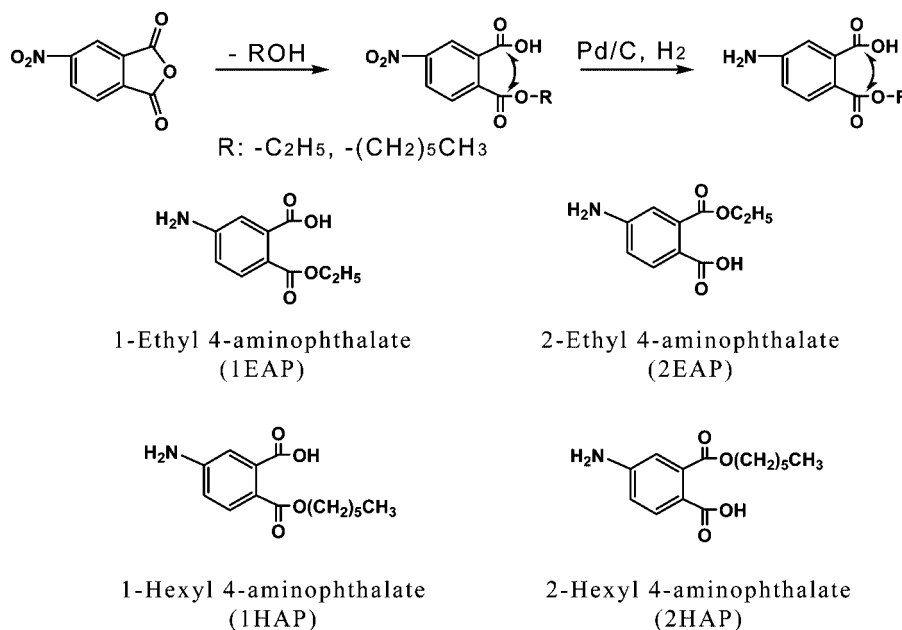
[†] Graduate School of Environmental Science.

[‡] Graduate School of Natural Science and Technology.

Scheme 1. Synthesis of PPI from 1- and 2-Alkyl 4-Aminophthalates



Scheme 2. Synthesis of Alkyl 4-Aminophthalates



scanning rate of $20\text{ }^{\circ}\text{C min}^{-1}$ in N_2 . Differential scanning calorimetry (DSC) was performed on a Perkin-Elmer DSC 7 at a scanning rate of $20\text{ }^{\circ}\text{C min}^{-1}$ in N_2 .

Synthesis. *1-Ethyl 4-Aminophthalate (1EAP) and 2-Ethyl 4-Aminophthalate (2EAP).* 4-Nitrophthalic anhydride (10 g, 0.052 mol) and dried ethanol (100 mL) were placed into a round-bottom flask. The reaction mixture was refluxed for 3 h. After being allowed to cool to $25\text{ }^{\circ}\text{C}$, 5% Pd/C (0.5 g) was added into the reaction mixture, and the mixture was stirred for 12 h in H_2 atmosphere. After filtration of Pd/C , ethanol was evaporated to afford the faint yellow

solid with the yield of 95.6%. The molar ratio of 1EAP and 2EAP was 57/43 estimated by 1H NMR.

The mixture of 1EAP and 2EAP was dissolved in ethyl acetate at $25\text{ }^{\circ}\text{C}$. *n*-Hexane was added into the solution with stirring. The precipitates were collected by filtration. The molar ratio of 1EAP and 2EAP in the precipitates was 93/7. The faint yellow solid was collected from the filtrate by evaporating the solvent. Then the obtained solids were dissolved in methanol at $25\text{ }^{\circ}\text{C}$. Water was added into the solution with stirring, and then the precipitates were collected by filtration. The molar ratio of 1EAP and 2EAP was

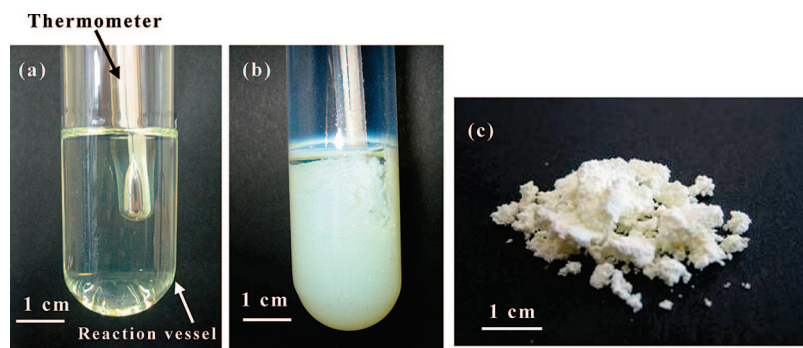


Figure 1. Photographs of the reaction mixture polymerized of 1EAP in DBT at a concentration of 2.0% for (a) 5 s and (b) 1 h and (c) fluffy PPI ribbons prepared for 6 h.

Table 1. Results of Polymerizations

run no.	polymerization conditions ^a		yield (%)	average size of ribbons		M_n^d ($\times 10^3$)	T_{10}^e ($^{\circ}\text{C}$)
	monomer ^b	conc (%)		length ^c (μm)	width (nm)		
1	1EAP	1.0	9.2	4.6	124	10.3	650
2		2.0	27.1	8.0	145	11.2	695
3		5.0	75.8	$>10^f$	138	3.3	709
4		10.0	83.5	$>10^f$	117	2.9	710
5	1EAP/2EAP (50/50)	2.0	23.0	9.5	134	9.3	703
6	2EAP	2.0	20.1	8.1	123	9.1	700
7	1HAP	2.0	27.5	9.5	139	6.6	667
8	1HAP/2HAP (50/50)	2.0	40.5	8.5	144	7.2	670
9	2HAP	2.0	42.4	8.3	149	9.5	693

^a Polymerizations were carried out at 330 $^{\circ}\text{C}$ in DBT for 6 h. ^b 1EAP = 1-ethyl 4-aminophthalate, 2EAP = 2-ethyl 4-aminophthalate, 1HAP = 1-hexyl 4-aminophthalate, and 2HAP = 2-hexyl 4-aminophthalate. Numbers in the parentheses were the mixing molar ratio. ^c Length from center part of aggregates of ribbons. ^d Number-average molecular weight estimated by end-group analysis with IR measurements. ^e Temperature of 10 wt % loss measured on a TGA with a scanning rate of 20 $^{\circ}\text{C min}^{-1}$ in N_2 . ^f Difficult to measure because of entanglements.

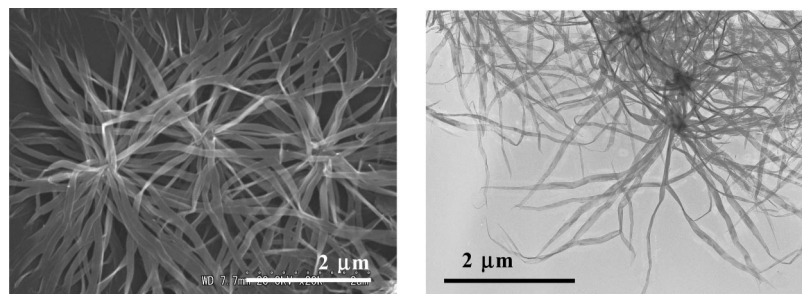


Figure 2. SEM and TEM images of PPI ribbons prepared from 1EAP at a concentration of 2.0% (run 2).

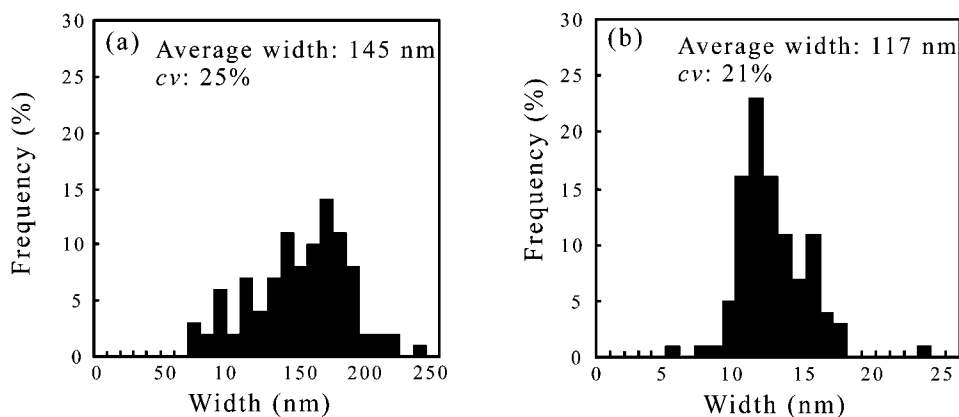


Figure 3. Distribution diagrams of width of PPI ribbons prepared from 1EAP at a concentration of (a) 2.0% (run 2) and (b) 10.0% (run 4).

29/71. These procedures were repeated several times to completely isolate the 1EAP and 2EAP, with the yields of 42.1% and 13.0%, respectively. 1EAP mp: 157 $^{\circ}\text{C}$. Anal. Calcd for $\text{C}_{10}\text{H}_{11}\text{O}_4\text{N}$ (209.20): C, 57.41; H, 5.30; N, 6.70. Found: C, 57.45; H, 5.01; N, 6.64. $^1\text{H NMR}$ (300 MHz, acetone- d_6): δ 11.16 (s, 1H), 7.61–7.59 (d, 1H, $J = 8.4$ Hz), 6.85–6.84 (s, 1H), 6.76–6.72 (d, 1H, $J = 8.4$ Hz), 5.49 (s, 2H), 4.24–4.17 (q, 2H, $J = 7.1$ Hz), 1.30–1.25 (t, 3H, $J = 7.1$ Hz). IR (KBr): 3456, 3359, 3236, 2997, 2976, 2688, 2337, 2214, 2125, 1900, 1703, 1633, 1608, 1568, 1541, 1523, 1495, 1441, 1398, 1373, 1342, 1292, 1277, 1249, 1149, 1114, 1068, 1018, 764, 640, 665, 649, 553. 2EAP mp: 174 $^{\circ}\text{C}$. Anal. Calcd for $\text{C}_{10}\text{H}_{11}\text{O}_4\text{N}$ (209.20): C, 57.41; H, 5.30; N, 6.70. Found: C, 57.55; H, 5.06; N, 6.68. $^1\text{H NMR}$ (300 MHz, acetone- d_6): δ 10.74 (s, 1H), 7.71–7.68 (d, 1H, $J = 8.4$ Hz), 6.75–6.70 (m, 2H), 5.55 (s, 2H), 4.27–4.20 (q, 2H, $J = 7.1$ Hz), 1.29–1.24 (t, 3H, $J = 7.1$ Hz). IR (KBr): 3469, 3378, 3234, 2983, 2871, 2651, 2530, 1711, 1685, 1654, 1637, 1606, 1562, 1516, 1412, 1344, 1371, 1250, 1159, 1065, 1018, 879, 858, 831, 804, 783, 613, 567.

1-Hexyl 4-Aminophthalate (1HAP) and 2-Hexyl 4-Aminophthalate (2HAP). 4-Nitrophthalic anhydride (10 g, 0.052 mol), triethylamine (1 mL), and dried *n*-hexanol (30 mL) were placed into a round-bottom flask, and the reaction mixture was heated at 70 $^{\circ}\text{C}$ for 6 h.

Oily product was obtained after evaporation of *n*-hexanol. The product was dissolved in methanol (120 mL), and then 5% Pd/C (0.5 g) was added into the solution. The reaction mixture was stirred at 25 $^{\circ}\text{C}$ for 8 h in a H_2 atmosphere. After filtration of Pd/C, the faint yellow solid was obtained by evaporating methanol with a yield of 76.3%.

1HAP and 2HAP were also isolated in the similar procedures of 1EAP and 2EAP, with the yields of 11.3% and 19.7%, respectively. 1HAP mp: 117 $^{\circ}\text{C}$. Anal. Calcd for $\text{C}_{14}\text{H}_{19}\text{O}_4\text{N}$ (265.30): C, 63.38; H, 7.22; N, 5.28. Found: C, 63.36; H, 6.51; N, 5.29. $^1\text{H NMR}$ (300 MHz, acetone- d_6): δ 7.62–7.59 (d, 1H, $J = 8.4$ Hz), 6.84–6.83 (s, 1H), 6.76–6.72 (d, 1H, $J = 8.4$ Hz), 5.52 (s, 2H), 4.18–4.13 (t, 2H, $J = 6.6$ Hz), 1.72–1.63 (br m 2H, $J = 6.6$ Hz), 1.45–1.26 (br m 6H), 0.90–0.86 (t, 3H, $J = 6.6$ Hz). IR (KBr): 3460, 3348, 3234, 3052, 2949, 2868, 2682, 2356, 2204, 2148, 1884, 1707, 1633, 1603, 1576, 1550, 1529, 1508, 1489, 1394, 1340, 1302, 1275, 1250, 1151, 1126, 951, 766. 2HAP mp: 184 $^{\circ}\text{C}$. Anal. Calcd for $\text{C}_{14}\text{H}_{19}\text{O}_4\text{N}$ (265.30): C, 63.38; H, 7.22; N, 5.28. Found: C, 63.42; H, 6.88; N, 5.29. $^1\text{H NMR}$ (300 MHz, acetone- d_6): δ 7.71–7.68 (d, 1H, $J = 8.4$ Hz), 6.75–6.70 (m, 2H), 5.55 (s, 2H), 4.21–4.16 (t, 2H, $J = 6.6$ Hz), 1.71–1.62 (br m 2H, $J = 6.6$ Hz), 1.43–1.27 (br m 6H), 0.89–0.85 (t, 3H, $J = 6.6$ Hz). IR (KBr): 3840, 3448,

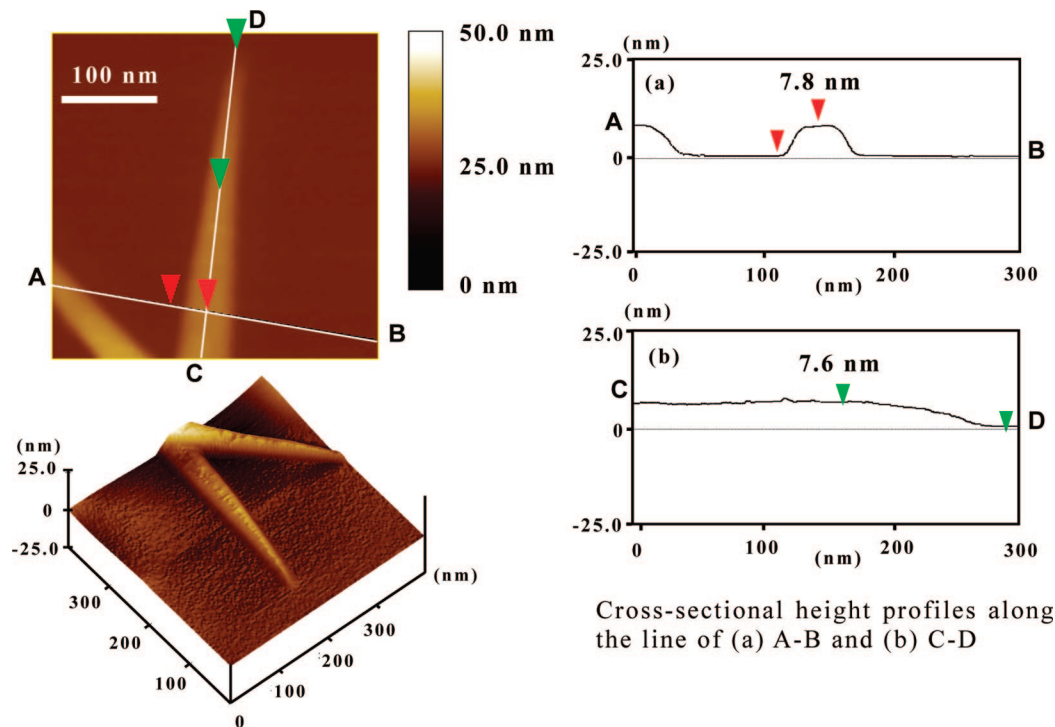


Figure 4. AFM height image of PPI ribbons prepared from 1EAP at a concentration of 2.0% (run 2).

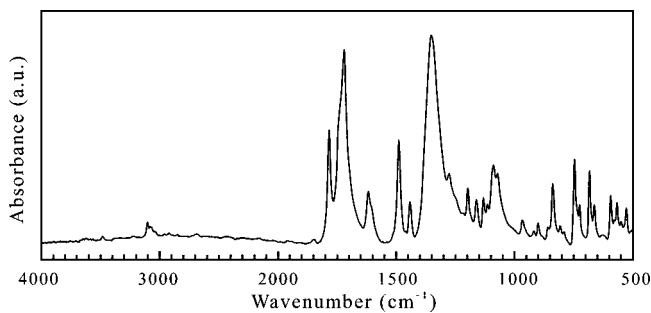


Figure 5. IR spectrum of PPI ribbons prepared from 1EAP at a concentration of 2.0% (run 2).

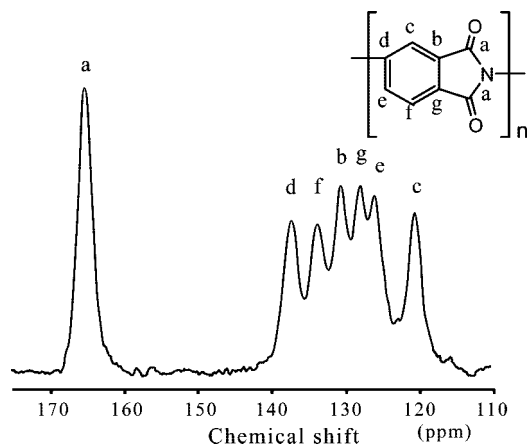


Figure 6. CP/MAS/TOSS ^{13}C NMR spectrum of PPI ribbons prepared from 1EAP at a concentration of 2.0% (run 2).

3361, 3253, 2952, 2858, 2667, 2573, 2541, 1705, 1660, 1599, 1560, 1514, 1456, 1421, 1350, 1300, 1273, 1259, 1163, 1146, 1066, 974, 953, 906, 864, 839, 804, 785, 615, 567.

PPI Dimer. 4-Aminophthalic acid (0.91 g, 5 mmol) was dissolved in DMF (13 mL), and consequently phthalic anhydride (0.89 g, 6 mmol) was added into the solution. Then, the reaction mixture was

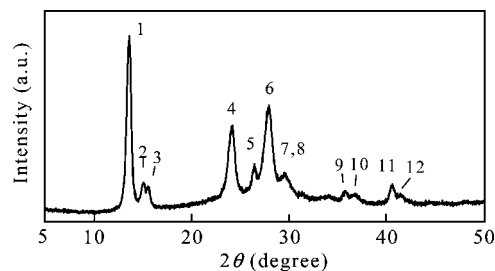


Figure 7. WAXS pattern of PPI ribbons prepared from 1EAP at a concentration of 2.0% (run 2). Peak numbers are corresponding to those in Table 2.

Table 2. Observed and Calculated Values of the Interplanar Spacing d from WAXS and ED Patterns

no. ^a	$d_{\text{obs}} \times 10 \text{ (nm)}$		$d_{\text{calc}} \times 10 \text{ (nm)}$	hkl
	WAXS	ED		
1	6.50		6.50	010
2	5.88	5.86	5.88	002
3	5.68		5.68	011
4	3.67	3.73	3.73	$\bar{1}00$
5	3.37		3.35	013
		3.33	3.30	$\bar{1}02$
6	3.19		3.19	111
7	3.02	2.95	3.00	102
8	3.02	2.96	3.00	004
9	2.51		2.50	023
10	2.44	2.47	2.43	$\bar{1}04$
11	2.22	2.20	2.19	104
			2.20	015
12	2.17		2.18	024

^a Peak numbers in Figures 7 and 8c.

stirred for 1.5 h at 25 °C. Pyridine (0.6 mL) and acetic anhydride (1 mL) were added into the reaction mixture, and the solution was stirred for 1.5 h at 25 °C. After pouring into cold water, precipitates were collected by filtration. The PPI dimer was obtained by the recrystallization from acetic anhydride with the yield of 81.2%; mp 266 °C. Anal. Calcd for $\text{C}_{16}\text{H}_7\text{O}_5\text{N}$ (293.23): C, 65.53; H, 2.41; N, 4.78. Found: C, 65.05; H, 2.35; N, 4.74. IR (KBr): 3103, 1853,

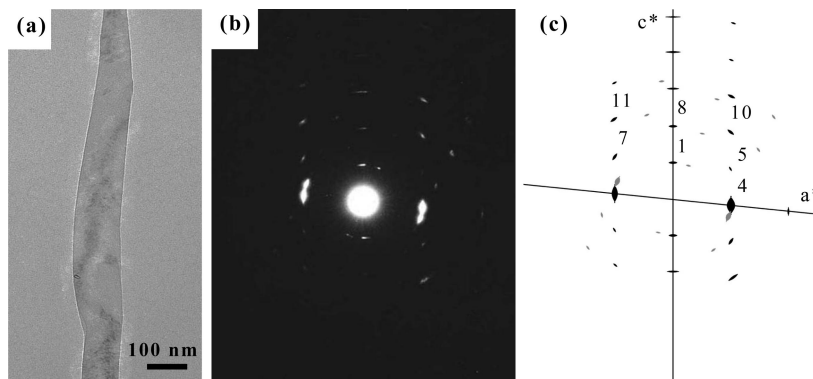


Figure 8. TEM image (a), ED pattern (b) obtained from one PPI ribbon, and its schematic drawing (c). Numbers of spots in (c) show corresponding peaks in Table 2.

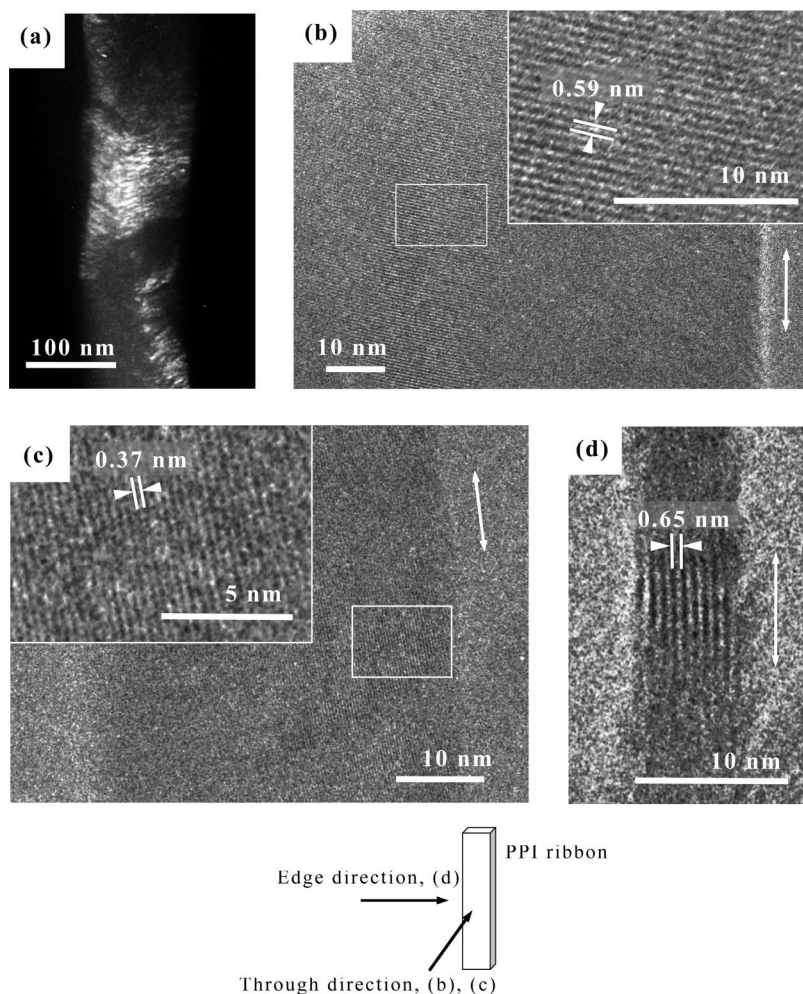


Figure 9. Dark-field image of PPI ribbons taken by using (002) reflection (a) and high-resolution TEM images of a ribbon incident to the through direction (b, c) and the edge direction (d). Arrows show the length direction of a ribbon.

1780, 1722, 1616, 1494, 1371, 1267, 1074, 881, 735, 710, 667. ^1H NMR (300 MHz, DMSO): δ 8.26–8.23 (d, 1H, J = 8.1 Hz), 8.17 (s, 1H), 8.10–8.07 (d, 1H, J = 8.1 Hz), 8.05–7.93 (m, 4H).

PPI Trimer. 4-Aminophthalic acid (0.44 g, 3 mmol) was dissolved in NMP (15 mL), and consequently PPI dimer (1.06 g, 3.6 mmol) was added into the solution. Then, the reaction mixture was stirred for 24 h at 25 °C. Pyridine (0.6 mL) and acetic anhydride (1 mL) were added into the reaction mixture, and the solution was stirred for 24 h at 25 °C. After pouring into cold water, precipitates were collected by filtration and dried under vacuum. The obtained solids were refluxed in acetic anhydride (20 mL) and filtered. The PPI trimer was obtained with the yield of 71.0%; mp 401 °C. Anal. Calcd for $\text{C}_{24}\text{H}_{10}\text{O}_7\text{N}_2$ (438.35): C, 65.76; H, 2.30; N, 6.39. Found:

C, 65.05; H, 2.36; N, 6.40. IR (KBr): 3103, 1859, 1782, 1724, 1618, 1493, 1375, 1263, 1076, 883, 741, 708. ^1H NMR (300 MHz, DMSO): δ 8.28–8.25 (d, 1H, J = 8.1 Hz), 8.22–8.19 (d, 1H, J = 8.1 Hz), 8.18 (s, 1H), 8.15 (s, 1H), 8.11–8.08 (d, 1H, J = 8.1 Hz), 8.05–8.02 (d, 1H, J = 8.1 Hz), 8.05–7.94 (m, 4H).

Preparation of PPI Ribbons. DBT (20 mL) was placed into a cylindrical flask equipped with gas inlet and outlet tubes and a thermometer and then heated up to 330 °C under a N_2 atmosphere. 1EAP (0.58 g, 2.8 mmol) was added into DBT at 330 °C, and the mixture was stirred to dissolve 1EAP. The stirring was stopped after 5 s, and then the polymerizations were carried out for 6 h. The solution became turbid after the addition of 1EAP due to precipitation of oligomers, and the faint yellow ribbon-like crystals

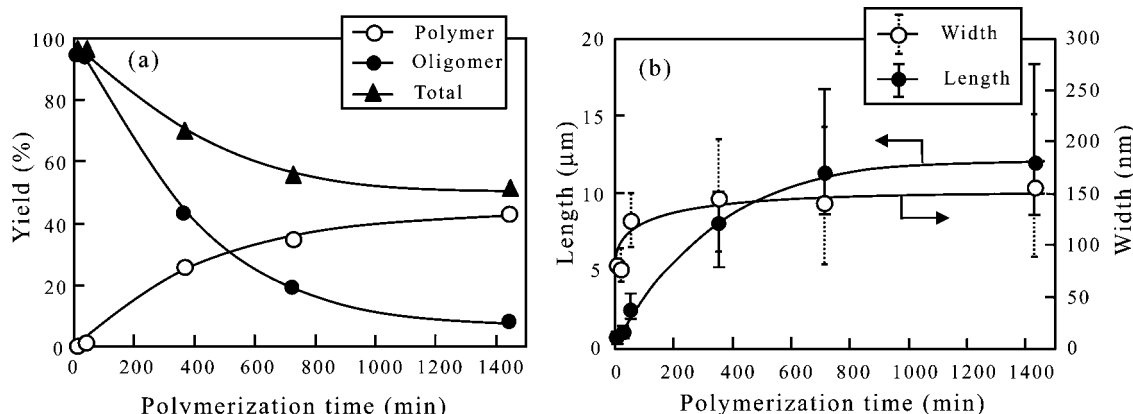


Figure 10. Plots of (a) yield of PPI ribbons, yield of oligomers collected from solution, and their total and (b) average length and width of PPI ribbons prepared from IEAP at a concentration of 2.0% as a function of polymerization time.

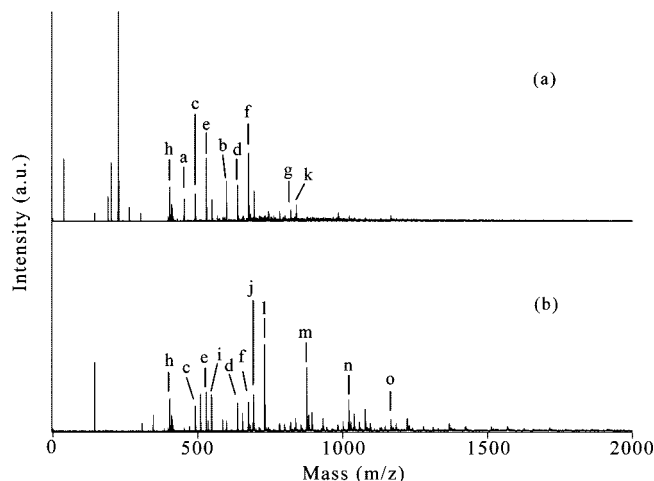


Figure 11. MALDI-TOF mass spectra of oligomers collected after 30 min. Samples were prepared by evaporation-grinding method with (a) dithranol and (b) 3-aminoquinoline as matrix and potassium trifluoroacetate. Polymerization of IEAP was carried out at a concentration of 2.0% in DBT at 330 °C.

were formed in the solution. The crystals were collected by filtration at 330 °C. They were washed with *n*-hexane, acetone, and methanol and dried at 50 °C under vacuum. The filtrate was allowed to cool to 25 °C and poured into *n*-hexane. The precipitates which were the oligomers dissolved in the solution at 330 °C were collected by filtration and washed with *n*-hexane.

Estimation of Number-Average Molecular Weight. Number-average molecular weight (M_n) was roughly estimated by using the absorbance ratio of the C=O of anhydride group and imide group recorded on IR spectra according to eq 1, which were obtained from PPI dimers and trimers.

$$M_n = \{0.21(\text{Abs}_{\text{imide}}/\text{Abs}_{\text{anh}}) + 1\} \times 145.1 \quad (1)$$

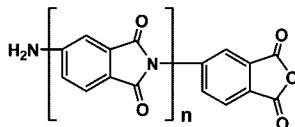
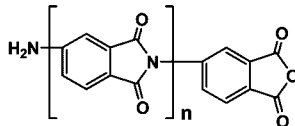
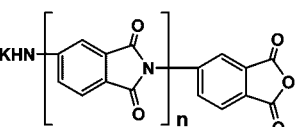
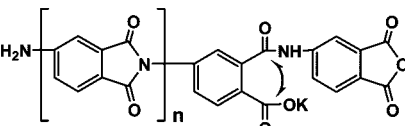
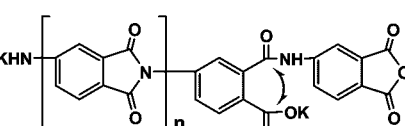
where $\text{Abs}_{\text{imide}}$ is the absorbance of imide C=O stretching and Abs_{anh} is the absorbance of anhydride ring symmetric C=O stretching.

Results and Discussion

The 1- and 2-alkyl 4-aminophthalates such as 1EAP, 2EAP, 1HAP, and 2HAP were synthesized from 4-nitrophthalic anhydride as shown in Scheme 2 and used as monomers of PPI. These monomers polymerize to form PPI by elimination of water and corresponding alcohol. There are three possible reaction routes as depicted in Scheme 1, but it is not clear which route occurs mainly at 330 °C.

First, IEAP was used as a monomer to control the morphology of PPI. Polymerizations of IEAP were carried out at a concentration of 1.0–10.0% in DBT at 330 °C without stirring. In this study, the concentration was described as the ratio of the theoretical polymer weight and the solvent volume. The solution became turbid by the precipitation of oligomers within 10 min, and then the fluffy crystals were obtained after 6 h as shown in Figure 1. Table 1 presents the polymerization results. The yields of the crystals were highly related to the concentration, and they were 9.2% and 83.5% at a concentration of 1.0% and 10.0%, respectively. They increased with the concentration. The concentration of 1.0% was too low to polymerize and induce the precipitation. The precipitated crystals exhibited the aggregates of ribbons as shown in Figure 2. The ribbons grew radially from the center part, and their tips became sharp. The length from the center of the aggregate to the tip and the width of each ribbon prepared at a concentration of 2.0% (run 2) was averagely 8 μm and 140 nm, respectively. The distribution diagram of the width of the ribbons prepared at a concentration of 2.0% (run 2) is shown in Figure 3. The coefficient variation (cv) was 25%. The thickness and the surface of the ribbons were observed by AFM as shown in Figure 4. The thickness was ~8 nm, and the surface was very smooth. The thickness became tapered along to the tip direction. As the concentration was higher, the length of the ribbons was inclined to become longer. Even though it was difficult to measure the length of ribbons because of the increase in the number of the ribbons from the center and the entanglement between ribbons at a concentration over 5%, the average length was longer than 10 μm. The average width was inclined to decrease with the concentration, and it was 117 nm at a concentration of 10% having the cv of 21% as also shown in Figure 2. It had been previously reported that the PPI was soluble only in concentrated sulfuric acid and methanesulfonic acid.¹⁵ However, the PPI ribbons obtained in this study were insoluble even in these strong acids. This insolubility of the PPI ribbons might be attributed to the high crystallinity and high molecular weight. Therefore, the chemical structure was analyzed by IR and solid-state ¹³C NMR spectroscopy. In the IR spectrum as shown in Figure 5, the absorption bands of imide bond such as C=O stretching and C–N stretching clearly observed at 1720, 1784, and 1352 cm⁻¹. In addition, there were no absorption bands of ester, carboxylic acid, and amide of the considerable intermediates. Because of the insolubility, the molecular weight could not be also determined by conventional methods such as gel permeation chromatography, NMR, viscosity measurement, and so on. M_n was estimated by end-group analysis with the IR spectrum in a similar procedure of poly(4-oxybenzoyl).¹⁶ The peak of carbonyl of anhydride linkage was slightly observed at 1853 cm⁻¹,

Table 3. Structural Assignment of Peaks in the MALDI-TOF Mass Spectra Reported in Figure 11

Structure	n	Mass (m/z)		Calculated	Peak
		Observed			Code
		Matrix			
		Dithranol	3-Aminoquinoline		
H^+ 	2	453.77	-	454.34	a
	3	599.27	-	599.46	b
K^+ 	2	491.85	491.91	491.45	c
	3	-	637.44	636.56	d
K^+ 	2	529.94	530.01	529.55	e
	3	675.47	675.61	674.66	f
	4	820.92	-	819.77	g
	0	403.61	402.92	402.46	h
K^+ 	1	-	548.08	547.57	i
	2	-	692.58	692.68	j
	3	839.96	-	837.79	k
	4	-	730.68	730.78	l
K^+ 	5	-	876.16	875.89	m
	6	-	1021.5	1021.0	n
	7	-	1167.0	1166.1	o

corresponding to the end group in Figure 5. Hence, M_n of the PPI crystals was approximately estimated from the absorbance ratio of the carbonyl groups in the anhydride to that in the imide linkages. They were in the range from 2.9×10^3 to 11.2×10^3 . In a CP/MAS/TOSS ^{13}C NMR spectrum of the PPI ribbons as shown in Figure 6, the seven peaks corresponding to the PPI structure were clearly observed. These results reveal the formation of high molecular weight PPI as precipitates.

The WAXS profile of the ribbons prepared at a concentration of 2.0% (run 2) and the ED pattern obtained from one ribbon are shown in Figures 7 and 8, respectively. Diffraction peaks were quite sharp, and the diffuse halo contributed from amorphous regions was hardly observed. The ribbons possessed quite high crystallinity. The ED pattern was not a fiber pattern

of cylindrical symmetry, and sharp diffraction spots were clearly observed. The fiber identity period on the meridian is nearly equal to the length of one repeating unit of PPI, and hereby it assumes that the chain axis is oriented parallel to the ribbon length. All diffractions in the ED pattern and the WAXS pattern could be assigned by the monoclinic lattice with parameters $a = 0.37$ nm, $b = 0.65$ nm, $c = 1.18$ nm, and $\beta = 96.0^\circ$, as shown in Figure 8c and Table 2. A dark-field electron micrograph of the ribbons was taken by using the (002) reflection as shown in Figure 9a. The crystal is not uniformly bright. The fine bright striations oriented in the horizontal direction are observed in many places. This fact suggests that some regions of internal distortions are present within the crystal. As aforesaid, the crystals are formed by the rapid

precipitation of oligomers, and this rapid growth might result in the internal distortions. A high-resolution bright field electron micrograph of the ribbon-like crystal was taken as shown in Figure 9b–d. From the micrograph incident to the through direction, lattice fringes can be distinguished running perpendicular as shown in Figure 9b and horizontal as shown in Figure 9c to the long axis of the ribbon. The spacing of the lattice fringes was measured directly from the image to be 0.59 and 0.37 nm, which corresponds to the interplanar spacing of (002) and (100) planes. From the micrograph incident to the edge direction, lattice fringes can be also distinguished running along the long axis of the ribbon, and the spacing of the lattice fringes was measured directly to be 0.65 nm, corresponding to the interplanar spacing of (010) plane. These results strongly indicated that the PPI molecules were aligned along the long direction of the ribbon.

In order to clarify the feature of the crystal growth, the yields of the ribbons and the oligomers collected from the solution and the sizes (average length and width) of the ribbons were plotted in the course of the polymerization of 1EAP at a concentration of 2.0% as shown in Figure 10. The yield of precipitates gradually increased with time, and it reached to 44.2% after 24 h. That of the oligomers recovered from the solution decreased correspondingly. The length also increased with time and it became 12 μm after 24 h. The width increased largely in the initial stage of polymerization and then became constant at 150 nm after 6 h. The thickness was constant at 8 nm through the polymerization. The ribbons grow mainly to the length direction by the consecutive supply of oligomers from solution. The oligomers recovered from the solution after 30 min were analyzed by MALDI-TOF mass spectrometry according to the previous reports.^{11,17} The spectra and the peak assignments are shown in Figure 11 and Table 3, respectively. The oligomers up to decamer were detected, and they were comprised of the imide linkage, not amide linkage. This fact means that the oligo(imide)s larger than the decamers would mainly be precipitated to form the crystals. Oligo(amic acid)s or oligo(amic acid ester)s, which were precursor of PPI as depicted in Scheme 1, prevent to form the crystals having clear habit because of the formation of hydrogen bonding and the structural catenation leading to the random sequence of *meta* and *para* linkages. The formation of the imide linkage avoids these disadvantages. The carbonyl absorption of anhydride linkages was detected as the end group of the oligomers, indicating that the polymerization mainly proceeded via the formation of the anhydride groups.

Chemical structure of oligomer end groups influences significantly the miscibility between the oligomer and the solvent, bringing about the drastic change in the morphology of the precipitated crystals.^{18,19} Further, copolymerization of the structural isomers lowers the crystallizability of oligomers due to the structural irregularity. However, it is expected that the difference in the structure of the alkyl 4-aminophthalate would not influence the morphology of PPI since the crystals are formed by the precipitation of the oligo(imide)s. Polymerizations of 2EAP, 1HAP, 2HAP, and the mixture of the isomers were carried out at a concentration of 2.0% in DBT at 330 °C. The results are also presented in Table 1. As expected, the PPI ribbons were formed from these polymerizations with the yields of 20.1–42.4% in spite of the difference in monomer structures and copolymerization. The average length and width were in the range of 8.1–9.5 μm and 134–149 nm, being comparable with those prepared from 1EAP under same conditions. Their thickness was ~ 11 nm. The values of M_n of these ribbons were in the range of 6.6×10^3 – 9.5×10^3 .

Thermal stability was evaluated on a TGA measurement in N_2 . All the products were quite stable, and weight loss was not observed up to 450 °C. Temperatures of 10% weight loss summarized in Table 1 were in the range of 650–710 °C, which was quite higher than the previously reported temperature of 580 °C.^{14,15} The obtained PPI ribbons exhibited excellent thermal stability. In the previous study, only the broad exotherm was detected at 550 °C on a differential thermal analysis.¹⁵ This exotherm was attributed to the thermal decomposition. In the case of the PPI ribbons, glass transition temperature and melting temperature were not observed under 650 °C on the DSC heating profile in N_2 . The PPI ribbons were thermally stable, and the exotherm previously reported was not detected. There were no thermal transitions under thermal decomposition temperature.

Conclusion

In conclusion, PPI nanoscale ribbons were prepared from 1EAP by using the reaction-induced crystallization of oligomers, which were approximately 12 μm in length, 150 nm in width, and 8 nm in thickness. They possessed quite high crystallinity, and the molecular chains aligned along the long axis of the ribbons. The oligo(imide)s were precipitated to form the ribbons, and the polymerization occurred in the ribbons to form high molecular weight PPI. Polymerizations of the other alkyl 4-aminophthalates such as 2EAP, 1HAP, 2HAP, and their isomeric mixtures also yielded the PPI nanoscale ribbons as well. The obtained ribbons exhibited excellent thermal stability.

Acknowledgment. The authors thank Dr. Yoshimitsu Sakaguchi and Mr. Takeshi Oohazama for useful discussions on NMR. This study was financially supported by 21st century center of excellence (COE) program of Okayama University, Japan, and a research grant from The Mazda Foundation.

References and Notes

- (1) Mittal, K. L. *Polyimides, Synthesis, Characterization, and Application*; Plenum Press: New York, 1984; Vol. 1.
- (2) Cassidy, P. E. *Thermally Stable Polymers, Syntheses and Properties*; Marcel Dekker: New York, 1980.
- (3) Nephew, J. B.; Nihei, T. C.; Carter, S. A. *Phys. Rev. Lett.* **1998**, *80*, 3276.
- (4) Tran-Cong, Q.; Harada, A. *Phys. Rev. Lett.* **1996**, *76*, 1162.
- (5) Kyu, T.; Lee, J. H. *Phys. Rev. Lett.* **1996**, *76*, 3746.
- (6) Williams, R. J. J.; Rozenberg, B. A.; Pascault, J. P. *Adv. Polym. Sci.* **1997**, *128*, 95.
- (7) Luo, K. *Eur. Polym. J.* **2006**, *42*, 1499.
- (8) Wang, X.; Okada, M.; Matsushita, Y.; Furukawa, H.; Han, C. C. *Macromolecules* **2005**, *38*, 7127.
- (9) Kimura, K.; Kohama, S.; Yamazaki, S. *Polym. J.* **2006**, *38*, 1005.
- (10) Yamashita, Y.; Kimura, K. *Polymeric Materials Encyclopedia*; CRC Press: Boca Raton, FL, 1996; p 8707.
- (11) Wakabayashi, K.; Uchida, T.; Yamazaki, S.; Kimura, K.; Shimamura, K. *Macromolecules* **2007**, *40*, 239.
- (12) Kimura, K.; Nakajima, D.; Kobashi, K.; Kohama, S.; Uchida, T.; Yamashita, Y. *Polym. J.* **2005**, *37*, 471.
- (13) D'Alello, G. F. US Patent 4,064,113.
- (14) Coudance, J.; Vert, J. *Eur. Polym. J.* **1987**, *23*, 501.
- (15) Philips, D. C.; Spewock, S. J. *Polym. Sci., Polym. Chem. Ed.* **1976**, *14*, 1137.
- (16) Kimura, K.; Horii, T.; Yamashita, Y. *J. Polym. Sci., Part A: Polym. Chem.* **2003**, *41*, 3275.
- (17) Gies, A. P.; Nonidez, W. K.; Anthamatten, M.; Cook, R. C.; Mays, J. W. *Rapid Commun. Mass Spectrom.* **2002**, *16*, 1903.
- (18) Kimura, K.; Kurihara, Y.; Ohmori, H.; Kohama, S.; Yamazaki, S.; Yamashita, Y. *Polymer* **2007**, *48*, 3429.
- (19) Kimura, K.; Nakajima, D.; Kobashi, K.; Kohama, S.; Uchida, T.; Yamashita, Y. *Polym. J.* **2005**, *37*, 471.

MA800874W